THE ASTROPHYSICAL JOURNAL, 244:115–123, 1981 February 15

FAR-INFRARED OBSERVATIONS OF THE CEPHEUS OB3 MOLECULAR CLOUD

NEAL J. EVANS II[1], E. E. BECKLIN[2], C. BEICHMAN[2], IAN GATLEY[3], R. H. HILDEBRAND[4,5,6], JOCELYN KEENE[5,6], M. H. SLOVAK[1], M. W. WERNER[3], AND S. E. WHITCOMB[4,6]
Received 1980 June 4; accepted 1980 August 25

ABSTRACT

The molecular cloud accompanying the Cepheus OB3 association has been observed in the infrared at wavelengths of 10–400 μm. Far-infrared emission at 55 μm and 125 μm from the two CO hot spots, Cep A and Cep B, was mapped with $\sim 1'$ resolution. Cep A was also mapped at 400 μm with $\sim 1'$ resolution. Both hot spots were searched for 20 μm sources. The Cep A hot spot appears to be heated by energy sources internal to the molecular cloud. The dust temperatures are sufficient to explain the gas temperatures if the dust heats the gas by collisions. In sharp contrast, the Cep B region appears to be heated from outside the cloud, with the strongest far-infrared emission arising near the interface between the molecular cloud and the S155 H II region. The gas heating rate through collisions with dust may be insufficient to achieve the gas temperature observed in Cep B.

Subject headings: clusters: associations — infrared: sources — interstellar: molecules

I. INTRODUCTION

The energetics of molecular clouds have recently become amenable to detailed study. Maps of carbon monoxide emission have shown that some regions in molecular clouds display gas kinetic temperatures of 20 K or more, in contrast to the $\sim$10 K temperatures which prevail over most of the typical molecular cloud. The existence of such hot spots implies the presence of local heating mechanisms. These local heat sources operate in addition to the global processes which maintain the rest of the molecular cloud at 10 K. While the total cooling rate of the gas through molecular line emission is generally modest, the energetic requirements of CO hot spots may still be substantial because most processes are inefficient at coupling energy into the gas. Collisions of gas particles with warm dust grains can heat the gas in regions of high density (Goldreich and Kwan 1974), but this mechanism requires that the dust temperature exceed the gas kinetic temperature. Consequently, a high dust cooling rate through far-infrared emission is predicted by this mechanism. Observations of this emission will supply a direct measure of the dust cooling rate and can thus test whether the mechanism is feasible. The total cooling rate can then be compared to known heat sources. In this paper we report infrared observations of two hot spots in the Cepheus OB3 molecular cloud; the observations supply a detailed test of theories of molecular cloud energetics.

The molecular cloud accompanying the Cepheus OB3 association has been studied in detail by Sargent (1977, 1979). The association has two subgroups. The younger of these two subgroups provides a number of late O and early B stars near the molecular cloud; these stars ionize the S155 H II region which lies to the north and somewhat behind the molecular cloud (Felli *et al.* 1978). While the molecular cloud as a whole is very large (20 pc $\times$ 60 pc), Sargent singled out several areas of special interest which have dimensions of $\sim$1–2 pc. One of these areas, designated Cep A, may be the birthplace of a new subgroup of the association (Sargent 1979). Subsequent studies of Cep A have located a 20 μm source of very low color temperature (Beichman, Becklin, and Wynn-Williams 1979), a group of H_2O masers (Blitz and Lada 1979), which coincide in position with several faint radio sources (Beichman *et al.*; Rodriguez *et al.* 1980*b*) and strong far-infrared emission (Koppenaal *et al.* 1979). In addition, a possible Herbig-Haro object has been reported near Cep A (Gyulbudaghian, Glushkov, and Denisyuk 1978), and Rodriguez *et al.* (1980*b*) have studied the region in the lines of several molecules and have found a Type I OH maser.

Another area of special interest, designated Cep B, is shown schematically in Figure 1. This region has the highest CO antenna temperature in the cloud, but

[1]Department of Astronomy, University of Texas at Austin.
[2]Institute for Astronomy, University of Hawaii.
[3]Department of Physics, California Institute of Technology.
[4]Department of Physics and Enrico Fermi Institute, University of Chicago.
[5]Department of Astronomy and Astrophysics and Enrico Fermi Institute, University of Chicago.
[6]Guest Observer, Mauna Kea Observatory, Institute for Astronomy, University of Hawaii.

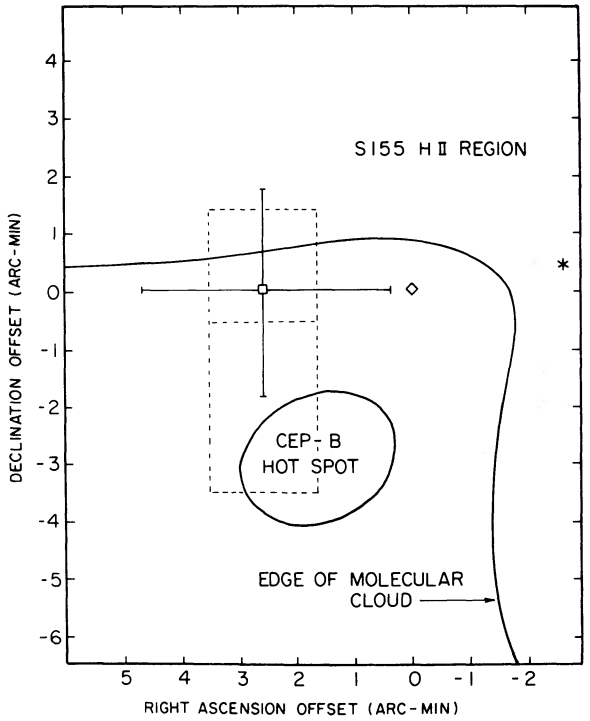

FIG. 1.—A schematic view of the Cep B region is presented. The boundary of the molecular cloud ($T_A^*(CO) = 5$ K) is shown by the solid curve. The S155 H II region extends throughout the region N and W of the molecular cloud. The nearest star of the younger subgroup (HD 217061) is shown near the right-hand edge of the map. The O7 star (HD 217086), which Felli *et al.* (1978) claim is the primary heat source for Cep B, lies about 6′ N of our (0,0) position. The diamond marks the compact radio source number 9 of Felli *et al.* The square is the position of GL 3000, with error bars shown. The dotted line encloses the area searched for 20 μm sources at a limiting flux density of 60 Jy. The lower section of the area was also searched at 10 μm to a limiting flux density of 10 Jy.

appears to be less dense than Cep A (Sargent 1979). The CO peak lies very near the edge of the cloud adjacent to the S155 H II region, which is excited by the stars of the younger subgroup. The high kinetic temperature seen toward Cep B may be caused by a newly formed star in the younger subgroup embedded in or lying behind the cloud (Sargent 1979). As evidence, Sargent cites the existence of a compact radio source (the diamond in Figure 1) and an infrared source GL 3000 (Price and Walker 1976) (the square with error bars) near the CO hot spot. Alternately, Felli *et al.* (1978) have suggested that Cep B is heated by visible stars of the association, primarily HD 217086, an O7 star, which lies 3.5 pc from the kinetic temperature peak. Felli *et al.* (1978) predict a far-infrared luminosity of $1.3 \times 10^4\ L_\odot$ from the Cep B region.

In this paper we report observations in several spectral regions defined as follows: far-infrared (30–300 μm), submillimeter (300–1000 μm), and middle-infrared (5–20 μm). We consider the implications of these observations for the energetics of hot spots in molecular clouds. The distance to the cloud is taken to be 725 pc (Crawford and Barnes 1970; Garmany 1973).

II. OBSERVATIONS

a) The Far-Infrared Observations

The far-infrared observations were made in 1979 May on the Kuiper Airborne Observatory with the University of Chicago six-detector dichroic photometer. This photometer uses a TlBr beamsplitter to make possible the simultaneous measurement of the flux in two broad spectral passbands at each of three colinear positions. The two passbands, 42–70 μm and 88–320 μm at half power, have flux-weighted mean wavelengths near 55 μm and 125 μm. The beams have diameters full width at half-maximum (FWHM) of 50″ and center-to-center separations of 75″. The corresponding long- and short-wavelength beams are coincident within ~7″. Further details concerning the instrumentation are given in Whitcomb *et al.* (1981).

Photometry was obtained at discrete points spaced at ~40″ intervals. Signals for each point were obtained by beam-switching. The chopper throw was 10′ in azimuth, corresponding to a nearly north-south direction (position angle ~155°–165°). Positions were determined by monitoring the location of field stars visually using a tracker camera; the uncertainty in determining the position of a strong source is estimated to be ±15″.

Flux densities were derived from observed signals, as described by Loewenstein *et al.* (1977), using assumed spectra of the form $\nu B(\nu, T)$, where $B(\nu, T)$ is the blackbody intensity. Corrections for atmospheric absorption were applied, based on the real-time H_2O vapor measurements in the direction of the telescope pointing. The average H_2O vapor column during the Cep A observations was 17 μm. The Cep B observations included data from two flights: on the first flight, the average H_2O column was 17 μm; on the second flight, it was 21 μm. The calibration object was Uranus for which we assumed brightness temperatures of 61 K and 59 K at 55 μm and 125 μm, respectively (Loewenstein and Harper, private communication; these temperatures are derived for a Uranian radius of 25,900 km). The flux densities were corrected to account for the extended nature of the source, as compared to Uranus. The relative sensitivities of the long-wavelength channels were calibrated to ~2%, and those of the short-wavelength channels to ~5%. Statistical uncertainties (1σ) for the Cep A observations (40 s integration time) were 140 Jy/beam at 55 μm and 40 Jy/beam at 125 μm. Varying integration times were used on the Cep B observations, resulting in 1σ uncertainties of 60–170 Jy/beam at 55 μm and 25–50 Jy/beam at 125

μm. Systematic uncertainties in the flux densities are estimated to be $\pm 20\%$, including the uncertainties in the Uranian brightness temperature. Because both wavelengths were measured simultaneously, ratios of flux density at 125 μm and 55 μm have systematic uncertainties of only $\pm 10\%$; nonetheless, this factor often dominates uncertainties in derived dust temperatures.

b) *The Submillimeter Observations*

The submillimeter observations of Cep A were made with the 2.2 m telescope of the Mauna Kea Observatory in 1979 July. The photometer, similar to that described by Hildebrand *et al.* (1977), used heat trap field optics. The spectral response of the system was determined by a metal mesh interference filter (Whitcomb and Keene 1980) at short wavelengths and by diffraction and the transmission of the field optics at long wavelengths; within this passband the detailed spectral response was determined largely by the atmospheric transmission, resulting in a flux-weighted mean wavelength of $\sim$400 μm. The beam diameter was 1.0 FWHM, and the source and reference beams were separated by 5′ in declination.

Photometry was obtained for individual points spaced by $\sim$40″ near the center of the map and $\sim$60″ in the outer regions. The positional uncertainty was $\pm 10''$. The noise was typically $\sim$6% of the peak signal. Atmospheric extinction was monitored by repeated observations of the peak signal.

Flux densities were derived assuming a source spectrum proportional to $\nu B(\nu, T)$. The calibration object was Mars. The Martian brightness temperature was assumed to be 215 K, based on the model described by Wright (1976). The peak 400 μm flux density for Cep A is 540 ± 120 Jy into a 1′ beam. The uncertainty is dominated by possible errors in the corrections for the difference between the source and calibration spectra and in the absolute calibration.

c) *The Middle-Infrared Data*

The regions around the CO hot spots in both Cep A and Cep B were searched for 20 μm sources and, to a more limited extent, 10 μm sources using the 2.2 m telescope of the Mauna Kea Observatory. A liquid-helium-cooled bolometer was used with filters spanning 7.8–25 μm (Dyck and Simon 1977). The beam was 7″ and the chopper spacing was 15″ in a north-south direction. Positions were determined to an accuracy of $\pm 3''$ by offsetting from nearby SAO stars. Further details on the observing technique may be found in Beichman (1979), and a discussion of the 20 μm source found in Cep A has been given by Beichman *et al.*

III. RESULTS

a) *Cep A*

The flux densities at 125 μm and 55 μm are presented for Cep A in Figure 2. Upper limits are 3σ. Positions are indicated by their offset in arcmin from the reference position, $\alpha(1950) = 22^h54^m21^s.7$; $\delta(1950) = +61°45'43''$, which was the peak of the 125 μm emission. This position, determined to $\pm 15''$, will now be compared with the positions of several other observations, starting with those of relatively large scale. Koppenaal *et al.* (1979) found three far-infrared sources in their scan across Cep A. Our map includes only the

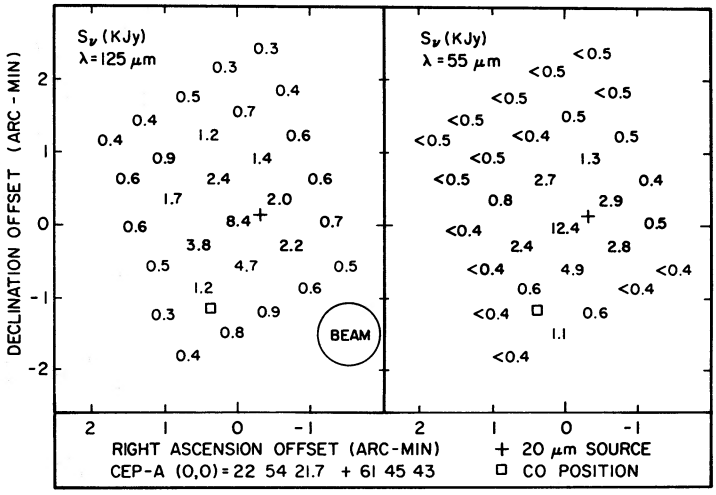

FIG. 2.—The Cep A flux densities in units of kJy ($=10^3$ Jy) are presented for wavelengths of 125 μm and 55 μm as indicated. The beam size is indicated in the left panel. The offsets are in arcmin with respect to the (0,0) position of $\alpha(1950) = 22^h54^m21^s.7$; $\delta(1950) = +61°45'43''$. In both panels, a plus sign marks the position of the 20 μm source reported by Beichman *et al.*, and a square marks the center position of the CO map of Sargent (1977). Upper limits to flux densities are 3σ.

region of the strongest far-infrared source, (FIRS1); it is FIRS1 which lies closest to the gas temperature and density peak of Cep A. The position of FIRS1, given by Koppenaal *et al.* (1979), is 2.4 east and 1.5 north of our position of peak emission, but their position agrees with ours to within their beam size of 4.5. The CO reference position given by Sargent (1977) is 0.4 east and 1.1 south (marked by a square in Fig. 2) of our reference position, but subsequent observations, discussed below, suggest that the center of molecular activity is closer to our position.

The 400 μm map is presented in Figure 3 in the form of contours of surface brightness, normalized to the peak. For comparison, a map of the 125 μm data is also presented in Figure 3, with contours normalized in the same way. The position of the peak emission at 400 μm agrees with that of the 125 μm emission to well within the uncertainties ($\pm 10''$ for the 400 μm data), but both positions differ from that of the 20 μm source (plus sign in Figs. 2 and 3) by $\sim 20''$. On the smallest scales, the 20 μm source is extended by about 9″ and is centered near a cluster of H_2O masers and compact

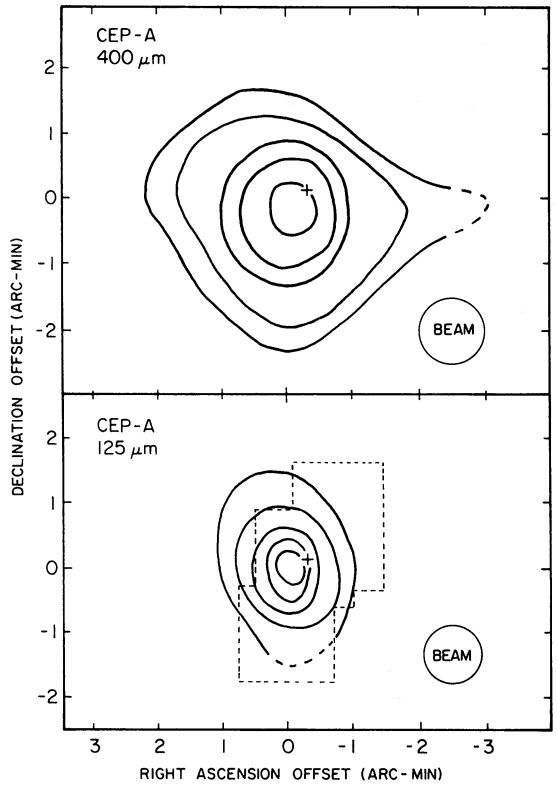

FIG. 3.—The top panel is the map of Cep A at 400 μm. The bottom panel is the map at 125 μm, and the area enclosed by the dotted line indicates the region searched at 20 μm to a limiting flux density of 30 Jy. The contours for both maps are drawn at 0.1, 0.2, 0.4, 0.6, and 0.8 of the peak flux density. The 20 μm source is indicated by the plus sign. The offsets follow the same convention as in Fig. 2.

H II regions (Beichman *et al.*; Rodriguez *et al.* 1980*b*). The 20 μm source was the only source found above 30 Jy in the region searched (indicated by the dotted line in Fig. 3). We shall refer to the 20 μm source and the compact H II regions collectively as the heating source in most of what follows.

The size of the emission region decreases with decreasing wavelength. This fact can be seen for $\lambda = 125$–400 μm directly from Figure 3, and the trend continues through 55 μm. This behavior is expected in a source where the dust temperature decreases with distance from the center. At 20 μm, Beichman *et al.* quote a source size of 9″, although more extended emission could have been missed with a 15″ chopper spacing.

The dust temperature (T_D) and optical depth at 125 μm (τ_{125}) have been calculated from the peak flux densities at 55 μm and 125 μm. The results are $T_D = 50$ K and $\tau_{125} = 0.08$. All grains within the beam and along the line-of-sight have been assumed to have the same T_D. The dust emissivity has been assumed to follow $\varepsilon = \varepsilon_o \lambda^{-\beta}$ between 55 μm and 125 μm, and T_D and τ_{125} were calculated for $\beta = 1$ (cf. Gatley *et al.* 1977, 1979). Use of $\beta = 2$ would result in T_D lower by 8–10 K.

b) Cep B

A map of S_ν (125 μm) in Cep B is presented in Figure 4, which also shows part of the T_A^*(CO) contours of Sargent (1977). The schematic view of the region, shown in Figure 1, can be used to locate the various objects of interest. The reference position, the peak of the 125 μm emission, is $\alpha(1950) = 22^h55^m08^s.7 \pm 15''$; $\delta(1950) = 62°21'30'' \pm 15''$. The positions of GL 3000 (Price and Walker 1976) and compact radio source 9 of Felli *et al.* (1978) are also indicated. The far-infrared emission is quite extensive, and our map is incomplete in the direction of the molecular cloud. The emission decreases more rapidly toward the S155 H II region, but the strongest emission arises near the interface between the molecular cloud and the H II region. The peak agrees in position with source 9 of Felli *et al.* The displacement of the peak emission position from the molecular hot spot contrasts sharply with the situation in Cep A.

Emission at 55 μm was detected only at four positions; consequently, the dust temperature structure is poorly defined. The positions with 55 μm detections are indicated in Figure 4 by letters, and the resulting T_D and τ_{125} (assuming $\beta = 1$) are given in the figure legend. The region enclosed by the dotted line in Figure 1 was searched for compact 10 μm and 20 μm sources. The search at 10 μm was confined to the lower section of the region. No source was found with $S_\nu(10\ \mu\text{m}) > 10$ Jy or with $S_\nu(20\ \mu\text{m}) > 60$ Jy. A better limit, $S_\nu(20\ \mu\text{m}) < 30$ Jy, was obtained for the upper 3′ of the region. For comparison, the source in Cep A has $S_\nu(10\ \mu\text{m}) = 0.8$ Jy and $S_\nu(20\ \mu\text{m}) = 48$ Jy.

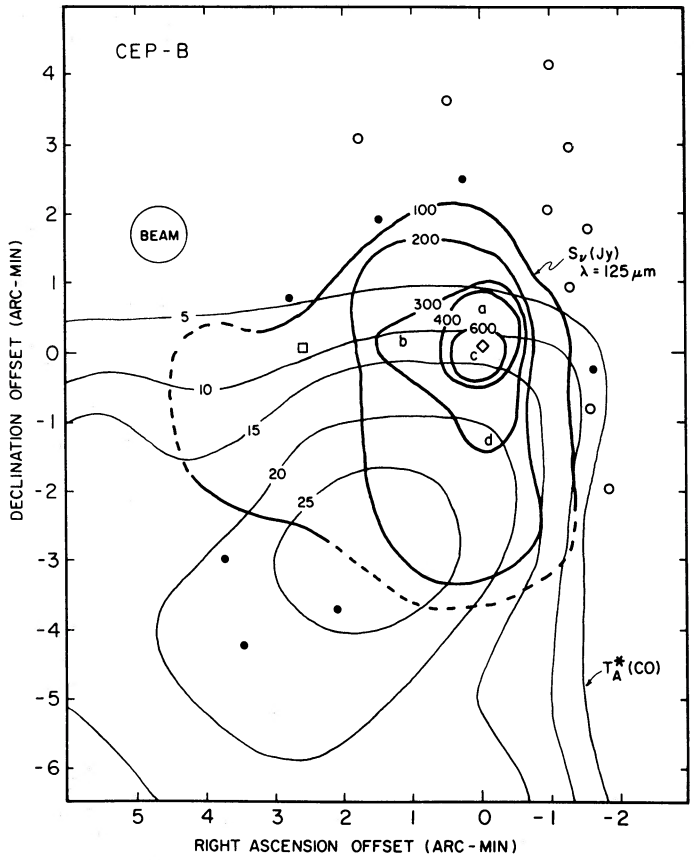

FIG. 4.—The far-infrared map of the Cep B region is presented. The offsets are in arcmin with respect to the (0,0) position of $\alpha(1950) = 22^h55^m08^s.7$, $\delta(1950) = +62°21'30''$. The heavy lines represent contours of equal S_ν (Jy) at $\lambda = 125$ μm in the Cep B region. The thin lines are contours of equal T_A^*(CO), taken from Sargent (1977). The square marks the position of GL 3000, and the diamond marks the position of compact radio source number 9 of Felli *et al.* (1978). The filled circles indicate positions of positive 125 μm detections outside the $S_\nu = 100$ Jy contour, and the open circles represent positions at which upper limits were obtained. The letters (a) through (d) mark positions where 55 μm emission was detected. At these positions, the following T_D and τ_{125} were obtained using a $\beta = 1$ emissivity law: (a) $T_D = 51 \pm 3$ K, $\tau_{125} = 5.7 \times 10^{-3}$; (b) $T_D = 41 \pm 4$, $\tau_{125} = 6.2 \times 10^{-3}$; (c) $T_D = 43 \pm 3$, $\tau_{125} = 1.2 \times 10^{-2}$; (d) $T_D = 39 \pm 3$, $\tau_{125} = 8.2 \times 10^{-3}$.

IV. THE CEP A REGION

a) The Energy Distribution and the Total Luminosity

The 55, 125, and 400 μm flux densities, integrated over the maps in Figures 2 and 3, are shown in Figure 5, along with the 85 and 150 μm flux densities from Koppenaal *et al.* (1979). The solid line in Figure 5 represents the expected emission from dust at $\langle T_D \rangle = 41$ K, radiating with a $\beta = 1$ emissivity law, and normalized to match the observations at 125 μm. This value of $\langle T_D \rangle$ is interpreted as an average over the map and along the line-of-sight; the corresponding average optical depth is $\langle \tau_{125} \rangle = 0.02$. The general consistency of our integrated fluxes with those of Koppenaal *et al.* indicate that our maps have not missed a substantial amount of emission. The middle-infrared flux densities, obtained at the position of the heating source, are also shown in Figure 5. Their position above the curve indicates the existence of warmer dust grains close to the heating source, just as the increased source size at 400 μm indicates the existence of cooler grains far from the heating source. Nonetheless, the assumptions of constant T_D and of $\beta = 1$ appear to provide a reasonable fit to the observations for λ from 20 to 400 μm. This situation is probably fortuitous.

The total luminosity of the Cep A region may be estimated by integrating the function which produced the solid curve in Figure 5. The result is $L = 2.5 \times 10^4 L_\odot$, in agreement with the results of Koppenaal *et al.* (1979). The primary contribution to the luminosity is the far-infrared emission which we attribute to warm dust grains in the molecular cloud. The tendency of the emission region to increase in size with increasing wavelength, together with the general symmetry around the peak position, indicates that the dust is being heated by an internal source. We believe that the 20 μm emission peak locates the position of the heating source.

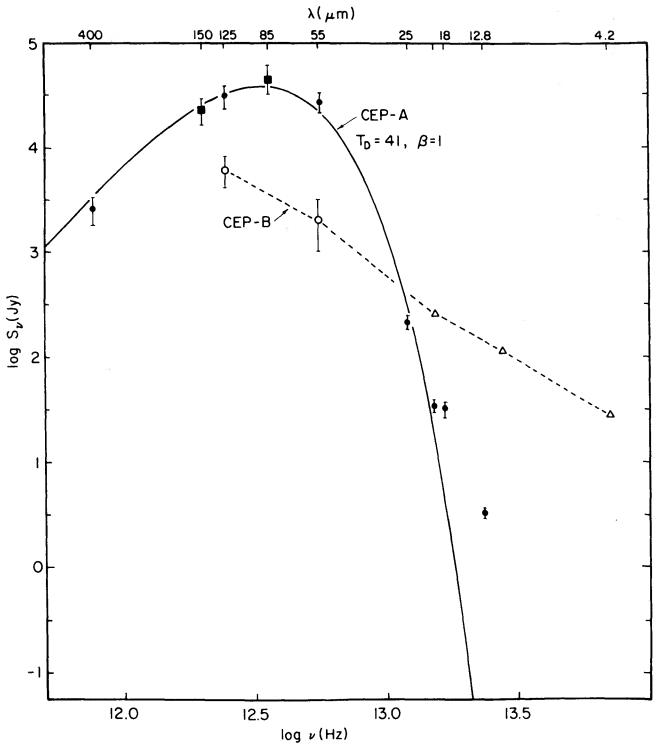

FIG. 5.—The energy distributions of Cep A and Cep B are presented. The Cep A points at 55, 125, and 400 μm were obtained by integrating the maps in Figs. 2 and 3. The points at 85 and 150 μm (filled squares) are taken from Koppenaal *et al.* (1979). The Cep A points at $\lambda \leq 25$ μm were obtained with 7″ diameter beam at the position of the 20 μm source (Beichman *et al.*). The solid line represents the emission from 41 K dust, radiating with a $\beta = 1$ emissivity law, and normalized to the observed S_ν at 125 μm. The Cep B data, connected by the dotted line, are values integrated over the map in Fig. 4 for $\lambda = 55$ and 125 μm. The middle-infrared data (open triangles) are taken from the data on GL 3000 (Price and Walker 1976).

The slight displacement of the peak far-infrared and submillimeter emission from the position of the heating source could result from density inhomogeneities.

The heating source may be a cluster of young stars and protostars. Beichman *et al.* found three compact H II regions requiring a total ionizing flux of $\sim 10^{45}$ Lyman continuum photons per second; if these are produced by three main sequence stars, the total stellar luminosity would be $0.8\text{–}2 \times 10^4 L_\odot$. Rodriguez *et al.* (1980*b*) interpret their data in terms of two compact H II regions, requiring a stellar luminosity of $0.7\text{–}1.8 \times 10^4$. In both cases, the lower end of the range is obtained using Panagia's (1973) calculations for a zero-age main sequence (ZAMS) star, while the upper end is based on calculations by E. Green (private communication). The approximate agreement of the observed total luminosity with the estimated stellar luminosity suggests that the stars ionizing the compact H II regions provide the energy for the infrared emission.

b) The Energetics of the Molecular Hotspot

In this section, we consider the energetics of the molecular hot spot. The gas kinetic temperature T_K will be compared to the values of T_D found above; the results will bear on models for heating molecular clouds. We begin by discussing the molecular line observations. Most of the detailed observations of molecular lines have been made at the reference position given in Table 2 of Sargent (1977). This position is 0.4 E and 1.1 S of the peak emission at 125 μm (0,0 position in Fig. 2). The $J = 1 \rightarrow 0$ CO line at this position is strongly self-reversed (Sargent 1977), and recent observations of the $J = 2 \rightarrow 1$ CO line with spatial resolution of ~35″ (Sargent, private communication) suggest that the self-absorption reaches its deepest point at a position 0.6 W and 0.1 S of our (0,0) position, and very close to the 20 μm position. The CO lines also show very broad wings (~20 km s^{-1} in extent, Loren *et al.* 1981) which are even broader (~50 km s^{-1}) near the 20 μm position (Rodriguez, Ho, and Moran 1980*a*; Loren 1981).

While self-reversed CO profiles of the type seen in Cep A are useful indicators of star forming regions, the self-reversal hinders the determination of gas kinetic temperature, T_K, because the self-reversal is formed by cooler material absorbing the radiation from the hot core of the cloud. Consequently, a calculation of T_K from the observed peak T_A^* gives only a lower limit to

the T_K in the cloud core. Using the data of Loren *et al.* (1981), taken at Sargent's original center position, we derive $T_K > 25$ K. The data with 35″ resolution from $J=2\rightarrow1$ CO closer to the 20 μm position (Sargent, private communication) give $T_K > 28$ K. Thus, $T_K/T_D > 28/50 = 0.6$ close to the 20 μm position. Such a close approach of T_K to T_D requires rather high densities, if the heating is assumed to be due to collisions of gas molecules with dust grains. From expressions in Goldsmith and Langer (1978), we find that at $T_K = 30$ K, the gas cooling rate is $\Lambda = 1.5\times10^{-22}$ ergs cm^{-3} s^{-1} at $n = 10^4$ cm^{-3}, and $\Lambda = 7.3\times10^{-22}$ ergs cm^{-3} s^{-1} at $n = 10^5$ cm^{-3}. The dust-gas heating rate is $\Gamma_{d-g} = 2.4\times10^{-33}\ T_K^{0.5} n^2\ (T_D - T_K)$ ergs cm^{-3} s^{-1}. The heating and cooling rates balance for $n > 4\times10^4$ cm^{-3} and $T_D = 50$ K. The required density is consistent with that found by Sargent (1977) from H_2CO observations. At the lower density of 10^4 cm^{-3}, inferred from ^{13}CO (Sargent 1977), the minimum cooling rate would be $\sim$6 times the heating rate. Because densities derived from ^{13}CO are likely to be underestimates in dense regions (cf. Evans 1980), we conclude that the collisions of gas particles with warm dust grains are a sufficient source of heat in the core of the Cep A hot spot.

c) *Dust and Gas Column Densities*

The relationship between dust and gas column densities is of interest to studies of energetics, gas-to-dust ratios, and chemical abundance gradients. In dense molecular clouds, the visual extinction is too high to be determined by star counting, but the optical depths derived from far-infrared and submillimeter emission can provide a measure of the dust column density. The gas column density can be estimated from N_{13}, the column density of ^{13}CO, if an abundance for ^{13}CO is assumed. Based on a variety of sources, Evans, Blair, and Beckwith (1977) found that the average far-infrared optical depth (τ_{FIR}) was related to N_{13} by $\tau_{FIR} = 10^{-18}\ N_{13}$, within a factor of 2. Toward Cep A, $N_{13} = 5-7\times10^{16}$ cm^{-2} (Sargent 1979). If we compare these with the peak τ_{125}, then $\tau_{125} = 1.1-1.6\times10^{-18}\ N_{13}$; using the average τ_{125} results in $\langle\tau_{125}\rangle = 3-5\times10^{-19}\ N_{13}$. These relations are consistent with that of Evans, Blair, and Beckwith (1977), given the uncertainties.

Because the dust emission is quite sensitive to variations in T_D, even at wavelengths as long as 125 μm, the presence of any temperature gradients along the line-of-sight will cause the far-infrared emission to sample a somewhat different region of the cloud than does the ^{13}CO emission. This problem should be less acute at longer wavelengths as the dust emission moves into the Rayleigh-Jeans region. For example, the map of 400 μm emission in Figure 3 shows an east-west broadening which is also seen in ^{13}CO (Sargent 1977), whereas the map at 125 μm does not show this effect. Consequently, comparison of dust optical depths in the submillimeter region with N_{13} may be less affected by temperature gradients. Righini-Cohen and Simon (1977) found that $\tau_{350} = 5.6\times10^{-19}\ N_{13}$ for the average of a group of molecular clouds. The data of Smith *et al.* (1979), for the region around OMC 2, result in $\tau_{400} = 5\times10^{-20}\ N_{13}$ when a $\beta = 1$ law is used. In the case of Cep A, we find that $\tau_{400} = 2-3\times10^{-19}\ N_{13}$ at the peak, and $\langle\tau_{400}\rangle = 1-2\times10^{-19}\ N_{13}$ for the average emission. $T_D = 50$ K was assumed at the peak, and $\langle T_D\rangle = 41$ K was used for the average emission. The values for Cep A fall between the two published estimates.

V. THE CEP B REGION

a) *The Energy Distribution and the Total Luminosity*

The flux densities integrated over the Cep B map are 6 kJy at 125 μm and 2 kJy at 55 μm. The former is a lower limit because the map is incomplete to the south and east. The latter represents the sum of the emission at the four positions with 55 μm detections and is thus likely to be a serious underestimate of the total flux density. The integrated flux densities at 55 μm and 125 μm are shown in Figure 5, along with the middle-infrared measurements of GL 3000 (Price and Walker 1976). The solid angle covered by our map is comparable to that used for the measurements of GL 3000, but positional and calibration uncertainties are substantial for GL 3000. Thus, the energy distribution is quite uncertain, but it appears to be broader than that of Cep A.

The luminosity of the Cep B region, estimated by integrating under the observed points in Figure 5, is $4\times10^3\ L_\odot$. Because about half the flux is due to emission between 55 and 125 μm, the luminosity is underestimated for the reasons discussed above, as well as for the neglect of emission at longer wavelengths.

The energetics of the Cep B region have been discussed in some detail by Felli *et al.* (1978). They find that the O7 star HD 217086 is primarily responsible for ionizing the S155 H II region. They further argue that HD 217086 and other nearby stars heat the dust in the molecular cloud. Their predicted far-infrared luminosity for the molecular cloud is $1.3\times10^4\ L_\odot$, about 3 times our observed luminosity. Because our observed luminosity is a lower limit to the actual luminosity, the discrepancy may not be significant.

Our observations of far-infrared emission are in general agreement with the picture of a cloud heated from the outside. In such a case, one would expect T_D to decrease from the H II region into the molecular cloud, as observed in the case of M17 (Gatley *et al.* 1979; Icke, Gatley, and Israel 1980). The highest T_D does occur nearest the edge of the molecular cloud (position a in Fig. 4), and the other three positions, lying farther inside the cloud, have T_D lower by $\sim$10 K.

The fact that the 125 μm emission peaks at the position of source 9 suggests that this source may also be a major heat source for the region. Felli *et al.* (1978) conclude that it is a thermal component and note that it coincides with the brightest part of an arc of nebulosity which outlines the interface between the molecular cloud and the H II region. Thus, it may represent only a dense condensation of the ionized gas, rather than a separate compact H II region, ionized by its own newly formed star. This picture is in agreement with the fact that near source 9, $\tau_{125} \sim 0.01$, the highest value of the four positions with τ measurements, while T_D is not enhanced. If source 9 is ionized by a separate star which is hidden in the nebulosity, then the ionizing photon flux implied by the radio data corresponds to about a B1 star. Such a star has a total luminosity similar to that which we observe. The only other possibly thermal compact component found by Felli *et al.* (1978) was source 15. This very weak source lies $\sim 7'$ E and $4'$ S of our reference position and is thus unlikely to be a significant heating source for the region we have studied. Thus, it appears that the dust in the molecular cloud is heated from the outside, either by the visible stars of the association or by a star which ionizes source 9 and lies near the edge of the molecular cloud.

The absence of 10 and 20 μm compact sources can be used to place a limit on the luminosity of objects embedded in the part of the molecular cloud which was searched. The limit depends on the temperature of the objects. For the region scanned at 10 μm, $L_{500} < 200\ L_\odot$, where L_{500} is the luminosity of a 500 K object. Likewise, the 20 μm upper limit leads to $L_{100} < 10^3\ L_\odot$. ($L_{100} < 700\ L_\odot$ over the upper $3'$ of the region.) Thus, it appears that the primary heat source is not buried in the part of the molecular cloud searched at 20 μm and 10 μm. Extension of the region searched to cover the entire far-infrared emission region would provide a good test of the picture in which the cloud is heated from the outside.

b) *The Energetics of the Molecular Hot Spot*

A model for the gas energetics in Cep B should explain the displacement of the far-infrared peak from the CO hot spot. Put another way, why does T_A^*(CO) not peak at the position of highest T_D, near the edge of the molecular cloud? Several effects may contribute to this displacement. First the gas heating rate Γ_{d-g} depends on n^2, while the cooling rate is less dependent on n (Goldsmith and Langer 1978); densities near the edge of the cloud are likely to be lower, causing T_K to differ from T_D by a larger amount. Second, the CO antenna temperature may not accurately reflect T_K near the edge of the cloud if the density falls below 10^3 cm^{-3}, the minimum necessary for thermalization of the CO rotational levels. Finally, the size of the beam used to map the CO was $2'.5$; thus, some beam dilution near the edge of the cloud may cause an underestimate of T_A^*(CO). Observations of CO with smaller beams would be of value in this region.

A quantitative test of gas heating by collisions with warm dust can also be made. If we take $T_D = 40$ K and $T_K = 30$ K, the heating and cooling rates will balance at $n = 6 \times 10^4$ cm^{-3}. No direct measure of n is available for Cep B, but Felli *et al.* derive $n = 10^4$ cm^{-3} from Sargent's (1977) ^{13}CO data, a ratio of $N/N_{13} = 2 \times 10^6$ (Scoville, Solomon, and Penzias 1975), and an assumption of spherical symmetry. Sargent (1979) derives $n = 3 - 4 \times 10^3$ cm^{-3} from the same data by using Dickman's (1978) value for $N/N_{13} = 5 \times 10^5$. Neither of these density estimates is high enough for the dust-gas heating to produce the observed T_K. The discrepancy would be resolved if the ^{13}CO observations underestimate n, as was the case in Cep A. However, one might then expect to see 2 mm H_2CO emission, and Sargent (1977) reports that none was found at the Cep B peak. Thus, the density does not appear to be sufficient for the gas to be heated only by collisions with dust grains. If the density can actually be measured, then more consideration of other heating mechanisms (e.g., shocks) would be appropriate.

VI. SUMMARY

We have studied in the infrared the molecular cloud accompanying the Cepheus OB3 association. With the objective of testing theories for the energetics of molecular clouds, we have observed two CO hot spots, Cep A and Cep B, at wavelengths from 10 to 400 μm. The two regions have quite different properties in the infrared; these differences appear to be caused by differences in the way that the regions are heated.

The far-infrared measurements of Cep A support a picture in which stars embedded within the molecular cloud are responsible for heating the surrounding dust to temperatures from 40 to 50 K. The dust temperatures are high enough that the gas can be heated by collisions with the dust grains. The observed gas temperatures can be reached at $n > 4 \times 10^4$ cm^{-3}, a density which is consistent with H_2CO observations.

In contrast, the Cep B region appears to be heated by stars outside the molecular cloud as suggested in a model by Felli *et al.* (1978). Our data are in general agreement with their model predictions, but some details may need revision. In particular, it may be hard to achieve the high gas temperatures seen in Cep B through collisions with dust grains, unless the density is somewhat higher than currently thought.

We are extremely grateful to the personnel of the NASA Kuiper Airborne Observatory and to the staff of the 2.2 m telescope at the Mauna Kea Observatory.

We thank A. I. Sargent and R. B. Loren for helpful discussions and communication of data prior to publication. We are grateful to D. A. Harper for the digital offset guider used on the KAO and to G. Forrester, K. Sellgren, and C. G. Wynn-Williams for assistance with the observations. N. J. E. wishes to express his appreciation to his colleagues for a smooth and fruitful introduction to far-infrared astronomy. We also thank the referee, L. Blitz, for a careful reading and helpful suggestions. J. K. and S. E. W. thank the Fannie and John Hertz Foundation for support. This work was supported by NASA grants NSG-2345 to the University of Texas at Austin, NGR 05-002-281 to the California Institute of Technology, NSG-2057 to the University of Chicago, and NASW-3159 to the University of Hawaii.

REFERENCES

Beichman, C. A. 1979, Ph.D. thesis, University of Hawaii.
Beichman, C. A., Becklin, E. E., and Wynn-Williams, C. G. 1979, *Ap. J.* (*Letters*), **232**, L47.
Blitz, L., and Lada, C. J. 1979, *Ap. J.*, **227**, 152.
Crawford, D. L., and Barnes, J. V. 1970, *A. J.*, **75**, 952.
Dickman, R. L. 1978, *Ap. J. Suppl.*, **37**, 407.
Dyck, H. M., and Simon, T. 1977, *Ap. J.*, **211**, 421.
Evans, N. J., II 1980, *IAU Symposium 87, Interstellar Molecules*, ed. B. Andrew (Dordrecht: Reidel).
Evans, N. J., II, Blair, G. N., and Beckwith, S. 1977, *Ap. J.*, **217**, 448.
Felli, M., Tofani, G., Harten, R. H., and Panagia, N. 1978, *Astr. Ap.*, **69**, 199.
Garmany, C. D. 1973, *A. J.*, **78**, 185.
Gatley, I., Becklin, E. E., Sellgren, K., and Werner, M. W. 1979, *Ap. J.*, **233**, 575.
Gatley, I., Becklin, E. E., Werner, M. W., and Wynn-Williams, C. G. 1977, *Ap. J.*, **216**, 277.
Goldreich, P., and Kwan, J. 1974, *Ap. J.*, **189**, 441.
Goldsmith, P. F., and Langer, W. D. 1978, *Ap. J.*, **222**, 881.
Gyulbudaghian, A. L., Glushkov, Yu. I., and Denisyuk, E. K. 1978, *Ap. J.* (*Letters*), **229**, L137.
Hildebrand, R. H., Whitcomb, S. E., Winston, R., Stiening, R. F., Harper, D. A., and Moseley, S. H. 1977, *Ap. J.*, **216**, 698.
Icke, V., Gatley, I., and Israel, F. P. 1980, *Ap. J.*, **236**, 808.
Koppenaal, K., Sargent, A. I., Nordh, L., van Duinen, R. F., and Aalders, J. W. G. 1979, *Astr. Ap.*, **75**, L1.
Loewenstein, R. F., *et al.* 1977, *Icarus*, **31**, 315.
Loren, R. B. 1981, in preparation.
Loren, R. B., Plambeck, R., Davis, J. H., and Snell, R. L. 1981, *Ap. J.*, submitted.
Panagia, N. 1973, *A. J.*, **78**, 929.
Price, S. D., and Walker, R. G. 1976, *Air Force Geophys. Lab. Rept.*, AFGL-TR-76-0208.
Righini-Cohen, G., and Simon, M. 1977, *Ap. J.*, **213**, 390.
Rodriguez, L. F., Ho, P. T. P., and Moran, J. M. 1980*a*, *Ap. J.* (*Letters*), **240**, L149.
Rodriguez, L. F., Moran, J. M., Ho, P. T. P., and Gottlieb, E. W. 1980*b*, *Ap. J.*, **235**, 845.
Sargent, A. I. 1977, *Ap. J.*, **218**, 736.
———. A. I. 1979, *Ap. J.*, **233**, 163.
Scoville, N. Z., Solomon, P. M., and Penzias, A. A. 1975, *Ap. J.*, **201**, 352.
Smith, J., Lynch, D. K., Cudaback, D., and Werner, M. W. 1979, *Ap. J.*, **234**, 902.
Whitcomb, S. E., Gatley, I., Hildebrand, R. H., Keene, J., Sellgren, K., and Werner, M. W. 1981, in preparation.
Whitcomb, S. E., and Keene, J. 1980, *Appl. Optics*, **19**, 197.
Wright, E. L. 1976, *Ap. J.*, **210**, 250.

E. E. Becklin: Institute for Astronomy, 2680 Woodlawn Drive, Honolulu, HI 96822

C. Beichman: Physics Department, Downs Laboratory 320–47, California Institute of Technology, Pasadena, CA 91125

Neal J. Evans II and M. H. Slovak: Department of Astronomy, The University of Texas at Austin, Austin, TX 78712

I. Gatley: UK Infrared Telescope Unit, 900 Leilani Street, Hilo, HI 96720

R. H. Hildebrand, J. Keene, and S. E. Whitcomb: Enrico Fermi Institute, 5630 S. Ellis Avenue, Chicago, IL 60637

M. W. Werner: M/S 245–6, NASA-Ames Research Center, Moffett Field, CA 94035